Front. Chem. China 2010, 5(3): 277–287
DOI 10.1007/s11458-010-0213-6

FEATURE ARTICLE

Self-assembly of bridged silsesquioxanes incorporated with conjugated organic functionalities

Li LI, Fangjing CAI, Xuemei SUN and Huisheng PENG (✉)

Key Laboratory of Molecular Engineering of Polymers of Ministry of Education, Department of Macromolecular Science and Laboratory of Advanced Materials, Fudan University, Shanghai 200433, China

Self-assembly of bridged silsesquioxanes with a chemical structure of $(RO)_3Si\text{-}R'\text{-}Si(OR)_3$ represents an efficient approach to design and to fabricate functional organic/inorganic nanocomposites. The desired functionalities are mainly incorporated into the R' with R of a hydrolysable alkoxide group such as CH_3 or CH_3CH_2. This feature article discusses two typical assembly approaches: self-directed assembly aiming at ordered solid materials and surfactant-directed assembly aiming at periodic mesoporous organosilica, with emphasis on the bridged silsesquioxanes in which conjugated functional organic groups are incorporated. The conjugated moieties are shown to be critical to the resulting assembly structure, morphology, and property. Self-assembly of three bridged silsesquioxanes based on polydiacetylene, perylene, and porphyrin has been detailed, respectively.

Keywords self-assembly, bridged silsesquioxane, conjugated, nanocomposite

1 Introduction

Organic/inorganic nanocomposites have continuously attracted increasing attentions in recent years due to their combined properties from both inorganic (e.g., rigidity, high surface area, thermal and mechanical stability) and organic components (e.g., optical, electrical, and magnetic functionality, porosity, and hydrophobicity) [1–5]. Particularly, these nanomaterials may also demonstrate some interesting and synergic properties from organic and inorganic parts [6–9]. A wide variety of structural, optical, magnetic, and electrical materials and many other advanced applications are possible as a result of the above unique and often superior properties [9–15]. In the case of optical nanocomposites, for instance, optical efficiency, mechanical strength, and sensing functionality [16] have been improved with maintained optical transparency [17]. For another instance in nature, nacre has been well known to be composed of organic and inorganic phases assembled together to form lamellar structures with much improved mechanical properties [18].

The used inorganic building blocks are mainly composed of carbon nanotubes, layered silicates, metal oxides, metal nanoparticles, or semiconductors, among which SiO_2 might have been most widely explored due to a broad spectrum of applications [19–21]. Three main synthetic approaches, blending, sol-gel processes, and in situ polymerization, have been extensively investigated. For the above methods, sol-gel processing is particularly useful to synthesize organic/inorganic materials in various forms. For instance, a xerogel (dry gel) will be formed after the drying of a gel in air, while an aerogel with porous structure may be produced if the solvent is removed by supercritical extraction. In this aspect, self-assembly of bridged silsesquioxanes (molecular structure of $(RO)_3\text{-}Si\text{-}R'\text{-}Si\text{-}(RO)_3$) represents a typical and efficient approach to design and fabricate silica-based hybrid materials based on a sol-gel process [20]. This methodology provides several advantages: (1) alkoxysilane substituents at each end of the bridged silsesquioxane improve the solubility of organic moieties, enabling their use in the solution-based processing; (2) collective molecular interactions from hydrolyzed silanols and the bridging groups provide driving force for the assembly of complicated structures. Morphologies such as thin films, particulate materials, and patterns printed on solid substrates by employing pen lithography and ink-jet printing have been previously reported; (3) A wide variety of

Received March 8, 2010; accepted April 20, 2010
E-mail: penghs@fudan.edu.cn

Table 1 Available R' groups in bridged silsesquioxanes with chemical structure of $(RO)_3Si\text{-}R'\text{-}Si(OR)_3$. The left numbers correspond to the related reference numbers.

(5) 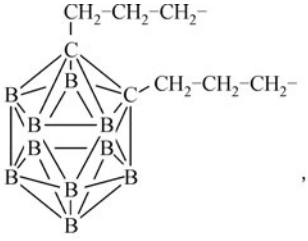

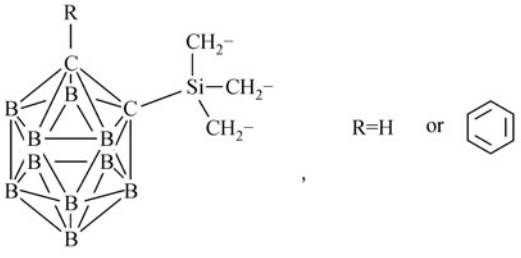

(11) $-(CH_2)_3-(CF_2)_4-(CH_2)_3-$

(12) 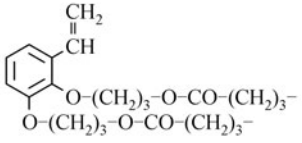

(13) 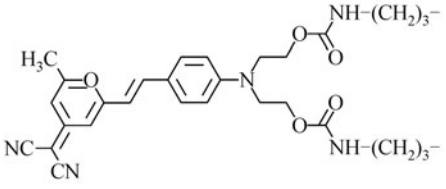

(14) 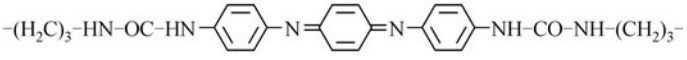

(15) 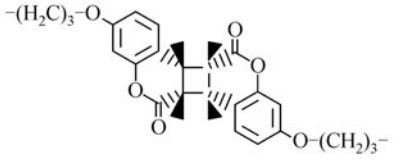

(28) $-(CH_2)_n-$, n=1, 2, 4, 6, 8, 10

(29) $-C\equiv C-$, $-CH_2-CH=CH-CH_2-$, $-C\equiv C-C\equiv C-$,

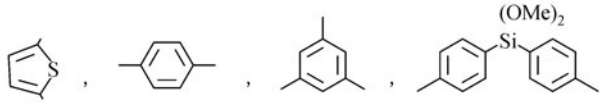

(30) $-(CH_2)_3-NH-CO-NH-(CH_2)_n-NH-CO-NH-(CH_2)_3-$
n=6, 8–12

(31) $-(CH_2)_3-NH-CO-O-CH_2-C\equiv C-C\equiv C-CH_2-O-CO-NH-(CH_2)_3-$,
$-(CH_2)_3-NH-CO-(CH_2)_8-C\equiv C-C\equiv C-(CH_2)_8-CO-NH-(CH_2)_3-$

(*Continued*)

(32) 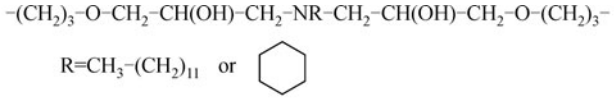

(33) 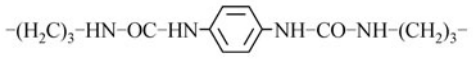

(34) 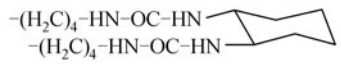

(35) 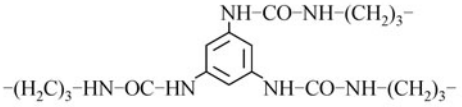

(36) 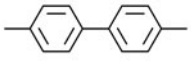

(37) 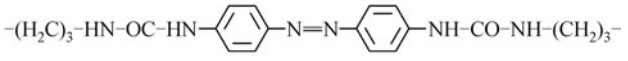

(38) 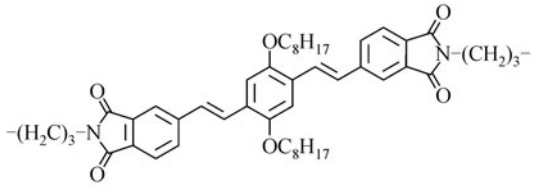

(39) 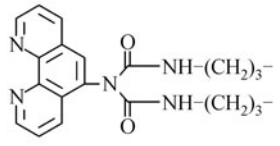

(40) 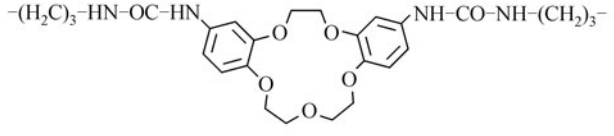

(41) 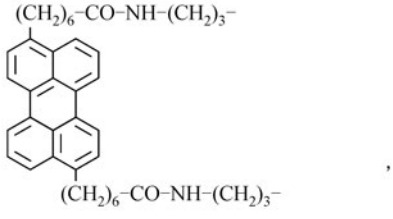

,

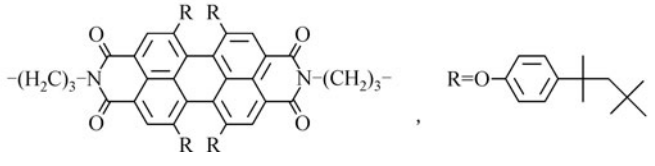

,

(*Continued*)

(42) 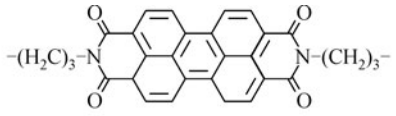

(43) 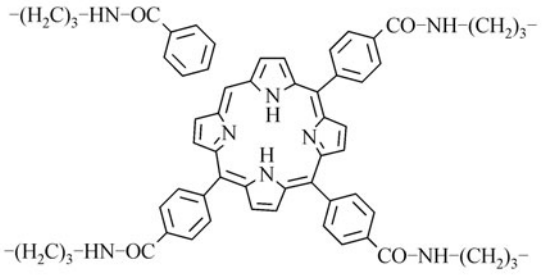

(44) 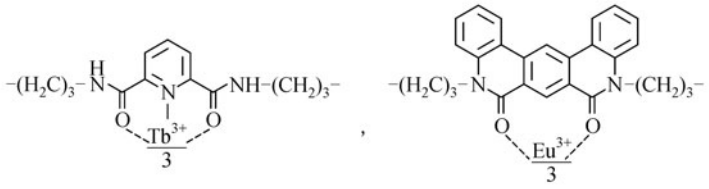

(45) 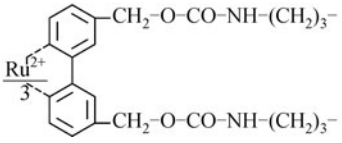

organic functionalities can be incorporated into the silica network, including phenyl, octyl, aminoalkyl, cyanoalkyl, thioloalkyl and vinyl groups (summarized in Table 1); (4) The inorganic silica framework improves the thermal stability of organic moieties and provides greater control over the alignment and electronic properties of organic chains.

There are mainly two approaches for self-assembly of bridged silsesquioxanes. Self-directed assembly exploits non-covalent interactions to form generally mesoscopically ordered lamellar solid materials. Figure 1 summarizes the typical structure of organic/inorganic nanocomposites by self-directed assembly of bridged silsesquioxane. The hybrid materials are normally prepared by spin coating (films) or using a precipitation process (powders). Another approach is surfactant-directed assembly, which allows the formation of periodic mesoporous organosilica after removal of surfactant molecules [22]. The structures of the above mesoporous materials can be tuned to be lamellar, hexagonal, or cubic by varying the experimental conditions [23–27].

A wide variety of organic/inorganic nanocomposites have been fabricated by self-assembly of bridged silsesquioxanes in the past two decades. Table 1 has shown chemical

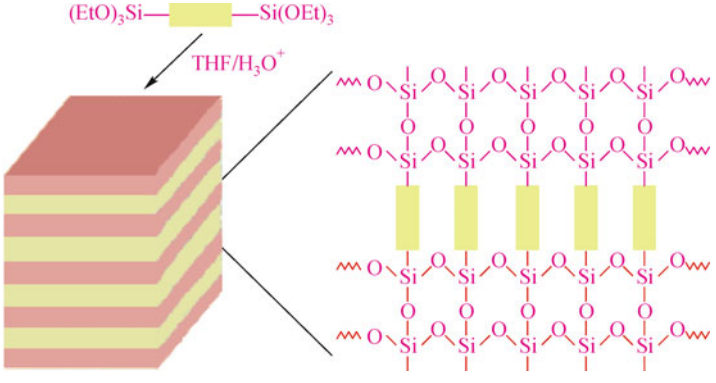

Figure 1 Formation of lamellar mesostructure by self-directed assembly of bridged silsesquioxane.

structures of some bridged silsesquioxanes [5,10–15,27–45]. However, the embedded organic components are mainly limited to passive functional groups, such as methylene, ethane, ethylene, dodecane, and benzene. Therefore, increasing attentions have been recently attracted to the incorporation of really functional organic groups, e.g., conjugated polymers, oligomers, or monomers. Here we mainly discuss three families of conjugated bridged silsesquioxanes derived from polydiacetylene, perylene, and porphyrin. The assembled nanomaterials have been explored as sensing and optoelectronic materials.

2 Chromatic polydiacetylene/silica synthesized from diacetylene-bridged silsesquioxanes

Polydiacetylene (PDA) has been extensively investigated as sensing materials due to the unique chromatic transition, typically from blue to red in response to environmental stimuli [46]. Various PDA materials such as vesicles, films, and nanocomposites have been fabricated, and their chromatic responses to a broad spectrum of external stimuli (temperature, pH, ion, solvent, stress, and ligand interactions) have been reported. A big challenge for PDA materials lies that the above chromatic responses mainly proceed in an irreversible way, which largely limits their practical applications as colorimetric sensors [47]. Several research groups have recently synthesized reversibly thermochromatic PDA vesicles and Langmuir-Schaefer films through strong hydrogen-bonding networks among PDA chains [48]. However, it remains challenging in the synthesis of robust PDA thin films with ready processing and good chromatic reversibility. A possible solution is to incorporate PDA into a robust silica network. The mechanically and thermally stable silica may provide the PDA with reversible thermochromatism at high temperatures. In this aspect, self-assembly of bridged silsesquioxane shed light on the efficient fabrication of high-quality PDA/silica composites.

A series of diacetylene-bridged silsesquioxanes have been used to synthesize the above composite materials [31]. In a typical synthesis, diacetylene-bridged silsesquioxanes were first dissolved in acidic solutions which were then coated on glass slides by spin-coating or dip-coating at room temperature; the resulting transparent colorless thin films were converted into blue PDA/silica films under UV irradiation. Figure 2 shows a typical transmission electron microscopy (TEM) image with lamellar mesostructure. The nanocomposite was synthesized from $(C_2H_5O)_3Si(CH_2)_3NHCO(CH_2)_8C{\equiv}CC{\equiv}C(CH_2)_8CONH(CH_2)_3Si(OC_2H_5)_3$, and the inter-lamellar distance corresponds to the length of the building molecule. The nanocomposite showed a reversible

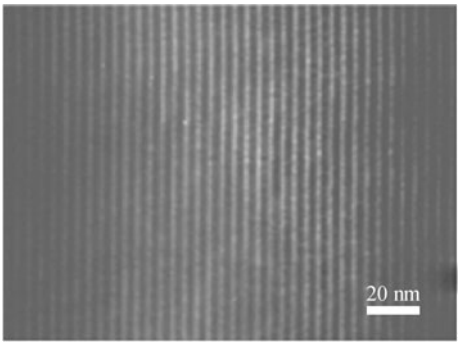

Figure 2 Transmission electron microscopy (TEM) image of polydiacetylene (PDA)/silica nanocomposites derived from self-directed assembly of $(C_2H_5O)_3Si(CH_2)_3NHCO(CH_2)_8C{\equiv}CC{\equiv}C(CH_2)_8CONH(CH_2)_3Si(OC_2H_5)_3$ in acidic THF solution. Reproduced with permission from Ref. [31]. Copyright 2005, American Chemical Society.

thermochromatism at high temperature, e.g., 113°C. Figures 3(a), 3(b), and 3(c) demonstrate the reversible chromatism with different color phases when heated at 90°C, and the color changes could be directly observed by the naked eyes. To quantitatively characterize the chromatic transition, the thermochromatism had been traced by UV-Vis spectrometer, which further confirmed the complete reversibility of chromatism in these nanocomposites.

Mesoporous PDA/silica nanocomposites had been also easily realized by co-assembly of above diacetylene-brdiged silsesquioxane and surfactants, e.g., cetyltrimethylammonium bromide (Figure 4(a)) [49]. The X-ray diffraction pattern in Figure 4(b) indicated a 2D hexagonally mesoporous structure in the nanocomposite. The TEM image in Figure 4(c) further confirmed the hexagonal mesostructure with a lattice constant of 5.7 nm. Similar to dense PDA/silica nanocomposites, the mesoporous PDA also reversibly responds to the thermal stimuli. Figure 5(a) showed a rapid and reversible thermochromatism at a high temperature of 103°C, and the above process could be performed for many cycles (Figure 5(b)). In Figure 5(b), the high colorimetric response values at high temperature and the near-zero values at room temperature indicated a complete blue-red-blue reversibility with practical applications as sensing materials. For both dense and mesoporous PDA materials, the reversible thermochromatisms at high temperatures were derived from excellent thermal stability provided by the robust silica framework. Figure 5(c) had compared the thermal stability of a pure PDA and a derived PDA/silica nanocomposite. The decomposition temperature of the PDA/silica had been improved ~250°C compared to the pure PDA. It should be noted that, due to the unique porous channel, the mesoporous PDA responded to chemicals much faster than the dense PDA (Figure 5(d)).

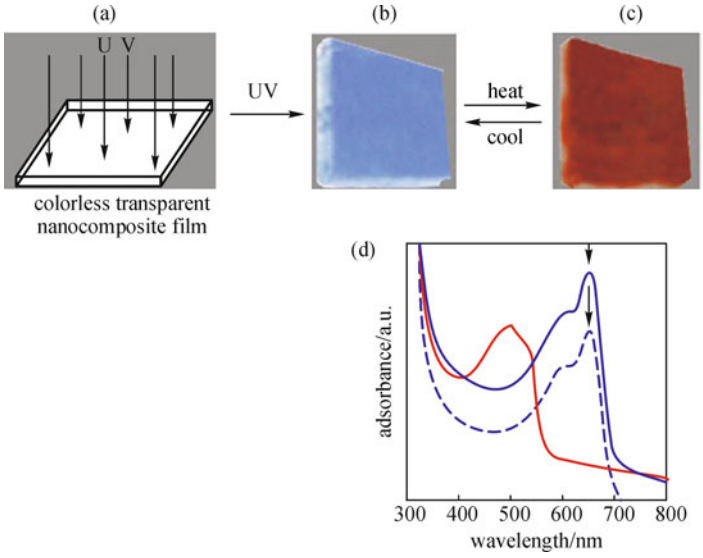

Figure 3 Thermochromatic properties of PDA/silica nanocomposites derived from $(C_2H_5O)_3Si(CH_2)_3NHCO(CH_2)_8CCCC(CH_2)_8CONH(CH_2)_3Si(OC_2H_5)_3$. (a) to (c) Schematic and photographs of PDA/silica films with different colors during the thermochromatic process. (d) UV-Vis spectra of the nanocomposite films subjected to a thermal cycle showing tunable chromatic reversibility. The solid blue line, solid red line and dashed line represent nanocomposites before thermal treatment, after heated at 90°C, and after cooled to room temperature, respectively. Reproduced with permission from Ref. [31]. Copyright 2005, American Chemical Society.

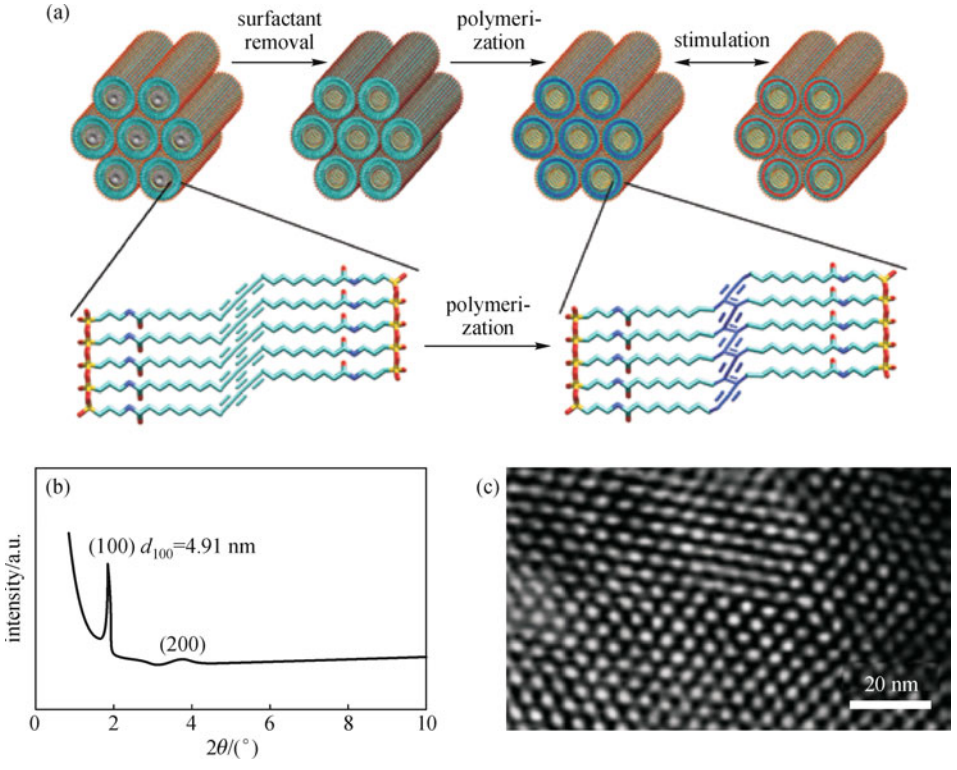

Figure 4 Mesoporous PDA/silica materials by co-assembling bridged silsesquioxane (structure of $(C_2H_5O)_3Si(CH_2)_3NHCO(CH_2)_8CCCC(CH_2)_8CONH(CH_2)_3Si(OC_2H_5)_3$) and surfactant (CTAB) followed by removal of CTAB. (a) Schematic illustration of the formation of chromatically mesoporous composites. (b) X-ray diffraction (XRD) pattern. (c) TEM image. Reproduced with permission from Ref. [49]. Copyright 2006, American Chemical Society.

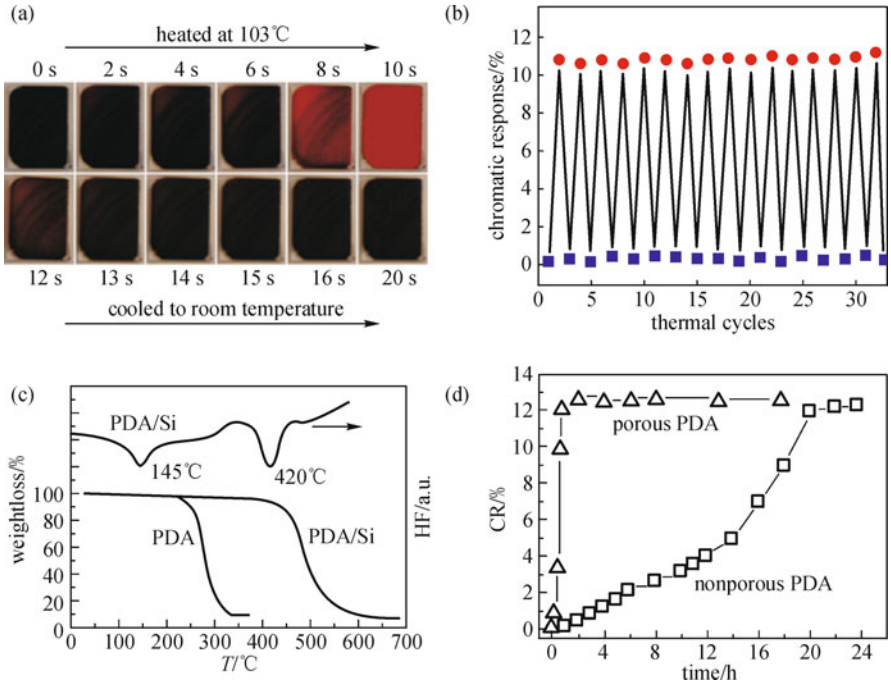

Figure 5 Chromatic properties of mesoporous PDA nanocomposites. (a) Photographs of rapid thermochromatic reversibility. (b) Chromatic response (CR) values at 25°C and 103°C for a series of thermal cycles. (c) DSC and TGA analysis. TGA of the corresponding polydiacetylenic acid is also shown. (d) CR values before and after removal of surfactant when exposed to a mixture of HCl and methanol. Reproduced with permission from Ref. [49]. Copyright 2006, American Chemical Society.

3 Self-assembly of perylenetetracarboxylic diimide bridged silsesquioxane

Perylene family has been most extensively studied as optoelectronic materials with promising applications in organic photovoltaic solar cells and sensing devices [50,51]. Due to the interesting molecule structure of conjugated macrocycle, perylene derivatives have been shown to have unique assembly behaviors [52]. For instance, Wahab [53] synthesized well-organized mesoporous organosilica films by co-assembly of 1,2-bis(triethoxysilyl)ethane and perylene-bridged silsesquioxane. The perylene-bridged silsesquioxane is located in the pore channel. Amphiphilic perylene bisimides had been shown to assemble into a wide variety of aggregates with tunable morphologies such as spheres, vesicles, and rods [54]. The above morphologies are dependent on the chemical structure of the building perylene derivatives, particularly the composition of side chains. Recently, we found that the hierarchical assembly of perylenetetracarboxylic diimide bridged silsesquioxane (PDBS) could also produce aggregates with tunable morphologies (tubes, fibers, or spheres) and sizes (micro-scale or macroscopic) (Figure 6) [55] by varying experimental conditions.

PDBS concentrations and evaporation speeds of solvents were concluded to play a key role in determining the assembly morphologies. High concentrations favored the formation of tubes or fibers, while low concentrations produced spheres. Micro-sized tubes or spheres were observed at high evaporation speeds, while macroscopic fibers were found with very slow evaporation of solvents. Interestingly, the macroscopic fibers were composed of micro-sized tubes. It seemed that the tubes further assembled into bigger fibers. As shown in Figure 6(g), the assembled aggregates had an ordered lamellar structure with an inter-lamellar distance equal to the length of the building bridged silsesquioxane.

A possible assembly mechanism had been summarized in Figure 7. It may take three steps during the formation of aggregates in Figure 6. (1) The building molecules stacked into small clusters due to strong π–π interactions and solvophobic interactions among perylenediimide moieties. (2) Small clusters further organized into nanoscale building blocks with various shapes and sizes, depending on the experimental conditions. (3) Nanoscale building blocks finally assembled to form micro-sized aggregates. The second and third steps are more critical during the assembly in this system, and they are closely related to the experimental conditions, such as PDBS concentrations and evaporation speeds. However, it remains challenging how micro-sized tubes assemble into macroscopic fibers.

A similar study on self-assembly of PDBS had been made

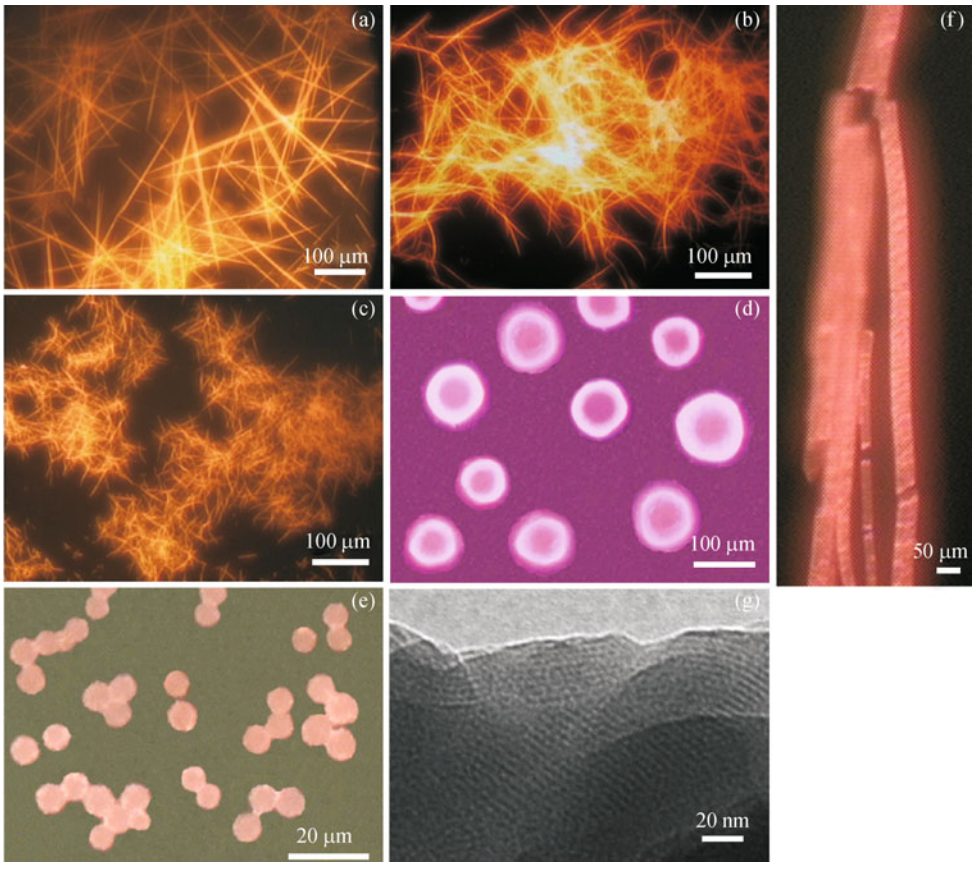

Figure 6 Fluorescent micrographs and TEM image of PDBS assemblies. (a) Evaporation of PDBS THF/petroleum ether (*v*/*v* of 1/5 and concentration of 8.3 mg·mL^{-1}) solution on glass at room temperature. (b) Coating PDBS THF/petroleum ether (*v*/*v* of 1/5 and concentration of 8.3 mg·mL^{-1}) solution on the hot glass with a temperature of ~65°C. (c) Coating PDBS THF/petroleum ether (*v*/*v* of 1/5 and concentration of 8.3 mg·mL^{-1}) solution on the hot glass with a temperature of 90°C. (d) Evaporation of PDBS THF/petroleum ether solution (*v*/*v* of 1/5 and concentration 2.7–3.3 mg·mL^{-1}) at room temperature. (e) Evaporation of PDBS THF/ H_2O solution (*v*/*v* of 1/5 and concentration 2.7–3.3 mg·mL^{-1}) at room temperature. (f) Very slow evaporation (air drying of two weeks) of PDBS THF/petroleum ether (*v*/*v* of 1/5 and concentration of 8.3 mg·mL^{-1}) solution. (g) TEM image of a tube at (a). Reproduced with permission from Ref. [55]. Copyright 2008, Wiley VCH.

by Luo et al. with the solvent of petroleum ether replaced by acetone [56]. Acetone is relatively a good solvent for perylenediimide parts compared to petroleum ether. Only tubes with lamellar mesostructure were observed. This is possibly because the solvent may largely affect the stacking of PDBS molecules during the assembly process.

4 Self-assembly of porphyrins-bridged silsesquioxane

Porphyrin derivatives have been systematically investigated for years as they show many excellent properties such as high chemical and thermal stabilities and great optoelectronic performances. Similar to perylene materials, due to the large and flat conjugated tetrapyrrole macrocycle, porphyrin-based assembly attracts increasing attentions in the field of chemistry and materials. A lot of assembly systems have been covered in the literature, in which porphyrins have been well known to form aggregates in forms of nanostructures including fibers, tubes [57], and sheets. Here we are interested in the assembly of porphyrin-bridged silsesquioxane to form useful uniform thin films. It was expected that the introduction of porphyrin moieties into the highly ordered silica network might provide the conjugated components with much improved optoelectronic and mechanical properties.

We have synthesized porphyrin-bridged silsesquioxane (PBS) with the chemical structure shown in Table 1 and further schematically illustrated in Figure 8 [43]. Unexpectedly, PBS molecules form thin films with highly ordered mesoporous structure after evaporation of acidic solution in THF (Figure 9(a)). The N_2 adsorption isotherms confirm the porous mesostructure with an average diameter of ~1.7 nm calculated through the BJH model. Normally, mesoporporous silica can be produced through co-assembly of silsesquioxane

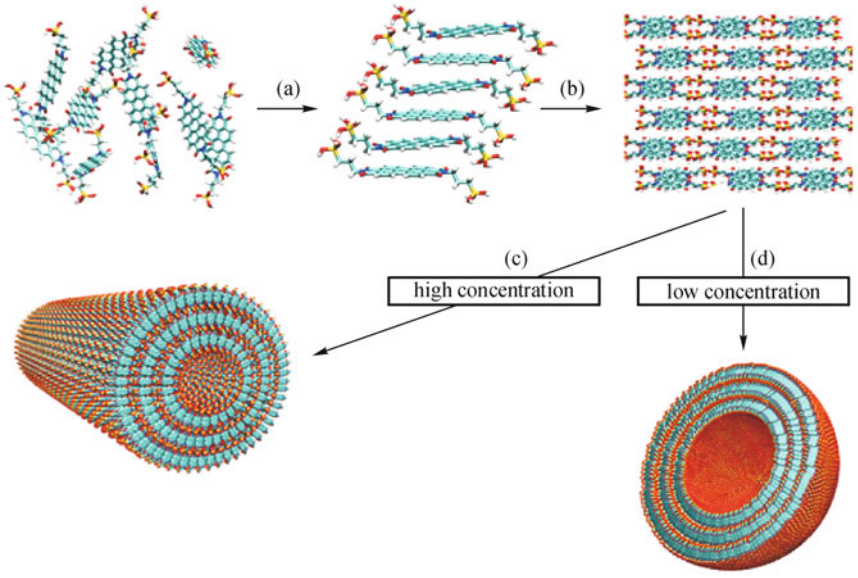

Figure 7 Schematic illustrations for (a) the proposed stacking of PDBS building molecules, (b) the formation of small cluster, (c) the assembly of clusters into tube, and (d) the formation of hollow spheres. Reproduced with permission from Ref. [55]. Copyright 2008, Wiley VCH.

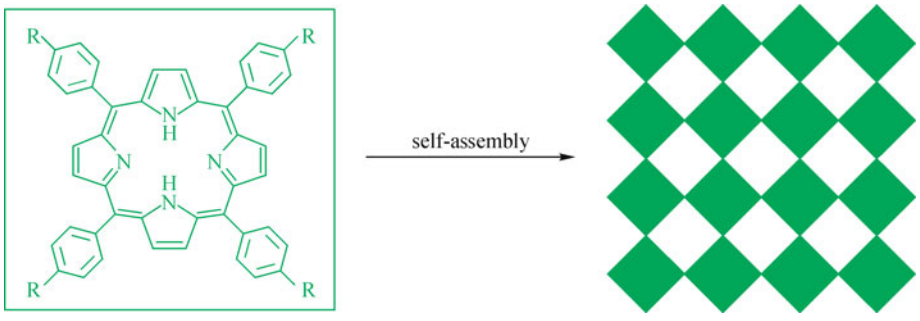

Figure 8 Schematic illustration of the formation of mesoporous structure by a square arrangement of PBS building molecules. Reproduced with permission from Ref. [43]. Copyright 2008, Wiley VCH.

and surfactant, followed by removal of the surfactant. Therefore, this approach may represent the first example for the synthesis of mesoporous materials by a directed assembly of organosilane without using any surfactant. It is easy and highly efficient with a neat one-step process, compared to the lengthy operation in a co-assembly approach. It may also provide an efficient synthetic paradigm to a family of functional porphyrin materials.

Further studies on the mesopores by atomic force microscopy showed that these uniform pores are square (Figure 9(b)). This square morphology may provide them with potential applications as separation media that combine both shape selectivity and enantioselectivity [58]. A side view of the above nanocomposite by TEM in Figure 9(c) further confirmed the ordered lamellar structure with an interlamellar distance of ~2.1 nm. As designed, the formation of highly ordered nanocomposites had greatly improved the optoelectronic performance of porphyrin moieties. The UV-Vis spectrometer showed that the absorption peaks for porphyrin rings shifted to the longer wavelengths. The red-shifted phenomenon indicated that porphyrin components have been more efficiently stacked with better energy transport in nanocomposites.

5 Conclusion

In this article, we have mainly covered the latest development in self-assembly of bridged silsesquioxanes, particularly those incorporated with conjugated organic functionalities. Three novel bridged silsesquioxanes based on polydiacetylene,

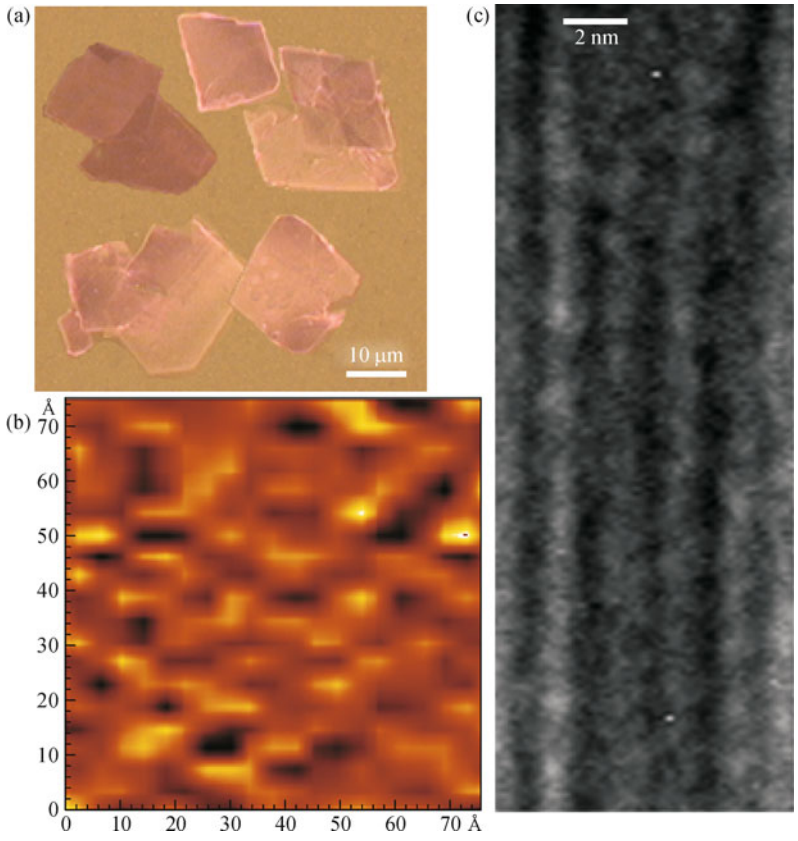

Figure 9 Flake-like and transparent porphyrin/silica nanocomposite films with a highly ordered mesostructure. (a) Optical microscopy image. (b) Atomic Force Microscopy (AFM) on side view of the squarely mesoporous structure of porphyrin/ silica nanocomposites. (c) TEM image of the nanocomposites. Reproduced with permission from Ref. [43]. Copyright 2008, Wiley VCH.

perylene, and porphyrin have been detailed, respectively. The conjugated organic groups are shown to be critical to the assembly structures, morphologies, and properties. Due to the formation of the robust silica framework, the resulting nanocomposites demonstrated excellent sensing, optoelectronic, and thermal properties.

Acknowledgements The work was supported by the National Natural Science Foundation of China (Grant No. 20904006), the Shanghai Committee of Science and Technology, China (Grant Nos. 1052nm01600 and 09PJ1401100), and Program for New Century Excellent Talents in University (Grant No. NCET-09-0318) and the Scientific Research Starting Foundation for Returned Overseas Chinese Scholars, Ministry of Education, China.

Li LI was born in Hunan Province in 1977. He received his Ph.D. degree in Materials Science and Engineering from Shanghai University in 2008 and is currently a postdoctoral fellow in the group of Prof. Huisheng Peng. His research centers on functional organic/inorganic nanocomposites.

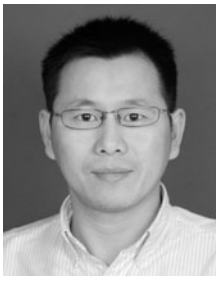

Huisheng PENG is a professor at Fudan University in the Key Laboratory of Molecular Engineering of Polymers of Ministry of Education, Department of Macromolecular Science, and Laboratory of Advanced Materials. His research focuses on functional polymer nanocomposites and polymer nanoparticles.

References

1. Lee, C. F.; Leigh, D. A.; Pritchard, R. G.; Schultz, D.; Teat, S. J.; Timco, G. A.; Winpenny, R. E. P., *Nature* **2009**, *458*, 314–318
2. Sofos, M.; Goldberger, J.; Stone, D. A.; Allen, J. E.; Ma, Q.; Herman, D. J.; Tsai, W. W.; Lauhon, L. J.; et al., *Nat. Mater.* **2009**, *8*, 68–75
3. Vendamme, R.; Onoue, S. Y.; Nakao, A.; Kunitake, T., *Nat. Mater.* **2006**, *5*, 494–501
4. Möller, S.; Perlov, C.; Jackson, W.; Taussig, C.; Forrest, S. R., *Nature* **2003**, *426*, 166–169
5. Gonza'lez-Campo, A.; Boury, B.; Teixidor, F.; Núñez, R., *Chem. Mater.* **2006**, *18*, 4344–4353

6. Meier, W., *Curr. Opin. Colloid Interface Sci*. **1999**, *4*, 6–14
7. Förster, S.; Plantenberg, T., *Angew. Chem. Int. Ed*. **2002**, *41*, 689–714
8. Förster, S.; Antonietti, M., *Adv. Mater*. **1998**, *10*, 195–217
9. Eckert, H.; Ward, M., *Chem. Mater*. **2001**, *13*, 3059–3060
10. Lim, M. H.; Stein, A., *Chem. Mater*. **1999**, *11*, 3285–3295
11. Zhao, L.; Clapsaddle, B. J.; Satcher, J. H.; Schaefer, D. W.; Shea, K. J., *Chem. Mater*. **2005**, *17*, 1358–1366
12. Elias, X.; Pleixats, R.; Man, M. W. C.; Moreau, J. J. E., *Adv. Synth. Catal*. **2006**, *348*, 751–762
13. Morais, T. D.; Chaput, F.; Lahlil, K.; Boilot, J. P., *Adv. Mater*. **1999**, *11*, 107–112
14. Guo, Y.; Mylonakis, A.; Zhang, Z.; Lelkes, P. I.; Levon, K.; Li, S.; Feng, Q.; Wei, Y., *Macromolecules* **2007**, *40*, 2721–2729
15. Zhao, L.; Vaupel, M.; Loy, D. A.; Shea, K. J., *Chem. Mater*. **2008**, *20*, 1870–1876
16. Sanchez, C.; Ribot, F.; Rozes, L.; Alonso, B., *Molec. Cryst. Liq. Cryst*. **2000**, *354*, 731–746
17. Wen, J.; Wilkes, G. L., *Chem. Mater*. **1996**, *8*, 1667–1681
18. Aksay, I. A.; Trau, M.; Manne, S.; Honma, I. I; Yao, N.; Zhou, L.; Fenter, P.; Eisenberger, P. M.; et al., *Science* **1996**, *273*, 892–898
19. Zou, H.; Wu, S.; Shen, J., *Chem. Rev*. **2008**, *108*, 3893–3957
20. Loy, D. A.; Shea, K. J., *Chem. Rev*. **1995**, *95*, 1431–1442
21. Hajji, P.; David, L.; Gerard, J. F.; Pascault, J. P.; Vigier, G., *J. Polym. Sci., B, Polym. Phys*. **1999**, *37*, 3172–3187
22. Heuer, A. H.; Fink, D. J.; Laraia, V. J.; Arias, J. L.; Calvert, P. D.; Kendall, K.; Messing, G. L.; Blackwell, J.; et al., *Science* **1992**, *255*, 1098–1105
23. Kresge, C. T.; Leonowicz, M. E.; Roth, W. J.; Vartuli, J. C.; Beck, J. S., *Nature* **1992**, *359*, 710–712
24. Vartuli, J. C.; Schmitt, K. D.; Kresge, C. T.; Roth, W. J. Leonowicz. M. E.; McCullen, S. B.; Hellring, S. D.; Beck, J. S.; et al., *Chem. Mater*. **1994**, *6*, 2317–2326
25. Beck, J. S.; Vartuli, J. C.; Roth, W. J.; Leonowicz, M. E.; Kresge, C. T.; Schmitt, K. D.; Chu, C. T. W.; Olson, D. H.; et al., *J. Am. Chem. Soc*. **1992**, *114*, 10834–10843
26. Zhao, D.; Feng, J.; Huo, Q.; Melosh, N.; Fredrickson, G. H.; Chmelka, B. F.; Stucky, G. D., *Science* **1998**, *279*, 548–552
27. Lu, Y.; Fan, H.; Doke, N.; Loy, D. A.; Assink, R. A.; LaVan, D. A.; Brinker, C. J., *J. Am. Chem. Soc*. **2000**, *122*, 5258–5261
28. Fan, H.; Reed, S.; Baer, T.; Schunk, R.; Lopez, G. P.; Brinker, C. J. Micro., *Micro. Meso. Mater*. **2001**, *44–45*, 625–637
29. Corriu, R. J. P.; Moreau, J. J. E.; Thepot, P.; Man, M. W. C., *Chem. Mater*. **1992**, *4*, 1217–1224
30. Moreau, J. J. E.; Vellutini, L. Dieudonné. P.; Man, M. W. C.; Bantignies, J. L.; Sauvajolb, J. L.; Bied, C., *J. Mater. Chem*. **2005**, *15*, 4943–4948
31. Peng, H.; Tang, J.; Pang, J.; Chen, D.; Yang, L.; Ashbaugh, H. S.; Brinker, C. J.; Yang, Z.; et al., *J. Am. Chem. Soc*. **2005**, *127*, 12782–12783
32. Romeo, H. E.; Fanovich, M. A.; Williams, R. J. J.; Mateˇjka, L.; Plesˇtil, J.; Brus, J., *Macromolecules* **2007**, *40*, 1435–1443
33. Moreau, J. J. E.; Pichon, B. P.; Man, M. W. C.; Bied, C.; Pritzkow, H.; Bantignies, J. L.; Dieudonné, P.; Sauvajol, J. L., *Angew. Chem. Int. Ed*. **2004**, *43*, 203–206
34. Karatchevtseva, I.; Cassidy, D. J.; Man, M. W. C.; Mitchell, D. R. G.; Hanna, J. V.; Carcel, C.; Bied, C.; Moreau, J. J. E.; et al., *Adv. Funct. Mater*. **2007**, *17*, 3926–3932
35. Pichon, B. P.; Man, M. W. C.; Dieudonné, P.; Bantignies, J. L.; Bied, C.; Sauvajol, J. L.; Moreau, J. J. E., *Adv. Funct. Mater*. **2007**, *17*, 2349–2355
36. Kapoor, M. P.; Yang, Q.; Inagaki, S., *J. Am. Chem. Soc*. **2002**, *124*, 15176–15177
37. Liu, N.; Yu, K.; Smarsly, B.; Dunphy, D. R.; Jiang, Y. B.; Brinker, C. J., *J. Am. Chem. Soc*. **2002**, *124*, 14540–14541
38. Dautel, O. J.; Wantz, G.; Almairac, R.; Flot, D.; Hirsch, L.; Lere-Porte, J. P.; Parneix, J. P.; Serein-Spirau, F.; et al., *J. Am. Chem. Soc*. **2006**, *128*, 4892–4901
39. Li,H.; Fu, L.; Liu, F.; Wang, S.; Zhang, H., *N. J. Chem*. **2002**, *26*, 674–676
40. Barboiu, M.; Cerneaux, S.; van der Lee, A.; Vaughan, G., *J. Am. Chem. Soc*. **2004**, *126*, 3545–3550
41. Schneider, M.; Hagen, J.; Haarer, D.; Müllen, K., *Adv. Mater*. **2000**, *12*, 351–354
42. Yang, L.; Peng, H. Huang, K.; Mague, J. T.; Li, H.; Lu, Y., *Adv. Funct. Mater*. **2008**, *18*, 1526–1535
43. Peng, H.; Lu, Y., *Adv. Mater*. **2008**, *20*, 797–800
44. Minoofar, P. N.; Dunn, B. S.; Zink, J. I., *J. Am. Chem. Soc*. **2005**, *127*, 2656–2665
45. Minoofar, P. N.; Hernandez, R.; Chia, S.; Dunn, B.; Zink, J. I.; Franville, A. C., *J. Am. Chem. Soc*. **2002**, *124*, 14388–14396
46. Sun, X.; Chen, T.; Huang, S.; Cai, F.; Chen, X.; Yang, Z.; Li, L.; Cao, H.; et al., *J. Phys. Chem. B* **2010**, *114*, 2379–2382
47. Peng, H.; Sun, X.; Cai, F.; Chen, X.; Zhu, Y.; Liao, G.; Chen, D.; Li, Q.; et al., *Nat. Nanotechnol*. **2009**, *4*, 738–741
48. Song, J.; Cisar, J. S.; Bertozzi, C. R., *J. Am. Chem. Soc*. **2004**, *126*, 8459–8465
49. Peng, H. S.; Tang, J.; Yang, L.; Pang, J.; Ashbaugh, H. S.; Brinker, C. J.; Yang, Z.; Lu, Y. F., *J. Am. Chem. Soc*. **2006**, *128*, 5304–5305
50. Cai, D.; Blair, D.; Dufort, F. J.; Gumina, M. R.; Huang, Z.; Hong, G.; Wagner, D.; Canahan, D.; et al., *Nanotechnology* **2008**, *19*, 1–10
51. Schneider, M.; Hagen, J.; Haarer, D.; Müllen, K., *Adv. Mater*. **2000**, *12*, 351–354
52. Liu, S. G.; Sui, G.; Cormier, R. A.; Leblanc, R. M.; Gregg, B. A., *J. Phys. Chem. B* **2002**, *106*, 1307–1315
53. Wahab, M. A.; Hussain, H.; He, C., *Langmuir* **2009**, *25*, 4743–4750
54. Zhang, X.; Chen, Z.; Würthner, F., *J. Am. Chem. Soc*. **2007**, *129*, 4886–4887
55. Peng, H.; Zhu, Y.; Peterson, D. E.; Lu, Y., *Adv. Mater*. **2008**, *20*, 1199–1204
56. Luo, Y.; Lin, J.; Duan, H. X.; Zhang, J.; Lin, C. K., *Chem. Mater*. **2005**, *17*, 2234–2236
57. Wang, Z.; Medforth, C. J.; Shelnutt, J. A., *J. Am. Chem. Soc*. **2004**, *126*, 15954–15955
58. Gier, T. E.; Bu, X.; Feng, P.; Stucky, G. D., *Nature* **1998**, *395*, 154–157